Original article

Alcides J. Sitoe, Franco Pretorius, Walter W. Focke*, René Androsch and Elizabeth L. du Toit

Solid–liquid–liquid phase envelopes from temperature-scanned refractive index data

https://doi.org/10.1515/polyeng-2021-0062
Received March 6, 2021; accepted April 20, 2021;
published online June 2, 2021

Abstract: A novel method for estimating the upper critical solution temperature (UCST) of *N*,*N*-diethyl-*m*-toluamide (DEET)-polyethylene systems was developed. It was validated using data for the dimethylacetamide (DMA)-alkane systems which showed that refractive index mixing rules, linear in volume fraction, can accurately predict mixture composition for amide-alkane systems. Furthermore, rescaling the composition descriptor with a single adjustable parameter proved adequate to address any asymmetry when modeling the DMA-alkane phase envelopes. This allowed the translation of measured refractive index cooling trajectories of DEET-alkane systems into phase diagrams and facilitated the estimation of the UCST values by fitting the data with an adjusted composition descriptor model. For both the DEET- and DMA-alkane systems, linear behavior of UCST values in either the Flory–Huggins critical interaction parameter, or the alkane critical temperature, with increasing alkane molar mass is evident. The UCST values for polymer diluent systems were estimated by extrapolation using these two complimentary approaches. For the DEET-polyethylene system, values of 183.4 and 180.1 °C respectively were obtained. Both estimates are significantly higher than the melting temperature range of polyethylene. Initial liquid–liquid phase separation is therefore likely to be responsible for the previously reported microporous microstructure of materials formed from this binary system.

Keywords: liquid–liquid phase diagram; mixing rule; polymer; refractive index; repellent.

1 Introduction

Knowledge of the phase behavior, at elevated temperatures, of polymer-mosquito repellent combinations is important for the optimization of long-life personal protective wear, e.g., textile-based socks [1], bracelets, and anklets [2]. For example, polymer-solvent phase separation can be exploited for the preparation of microporous strands suitable for long-life insect repellent anklets [2, 3]. The process relies on temperature induced phase separation (TIPS) [4–6]. The microstructure of the final product depends on the phase behavior of the system and the rate of cooling to which the material is subjected. The formation of a microporous polymer structure, capable of trapping large amounts of the liquid repellent internally, critically depends on phase separation induced by rapid cooling into the spinodal region. Furthermore, the cooling must start from a fully homogeneous solution of the repellent in the polymer melt. Therefore, it is important to know what the upper critical solution temperature (UCST) of the repellent-polymer system is. Above this temperature, equilibration will always yield a fully homogeneous solution. This means that the polymer processing temperature should exceed the UCST before the forced rapid cooling step commences.

It is not always clear whether the phase separation in systems containing crystallizable polymers initiates via liquid–liquid phase separation or via polymer crystallization. In a series of papers [7–11], it was suggested that phase separation of solutions containing *N*,*N*-diethyl-*m*-toluamide (DEET) and crystallizable poly(lactic acid) or poly(butylene succinate) proceeded via polymer crystallization. In contrast, Akhtar and Focke [3] assumed that it commences via liquid–liquid phase separation in the

***Corresponding author: Walter W. Focke**, Department of Chemical Engineering, UP Institute for Sustainable Malaria Control & MRC Collaborating Centre for Malaria Research, University of Pretoria, Private Bag X20, Hatfield 0028, Pretoria, South Africa, E-mail: walter.focke@up.ac.za. https://orcid.org/0000-0002-8512-8948
Alcides J. Sitoe, Franco Pretorius and Elizabeth L. du Toit, Department of Chemical Engineering, UP Institute for Sustainable Malaria Control & MRC Collaborating Centre for Malaria Research, University of Pretoria, Private Bag X20, Hatfield 0028, Pretoria, South Africa. https://orcid.org/0000-0001-8781-3378 (A.J. Sitoe). http://orcid.org/0000-0001-5579-1231 (E.L. du Toit)
René Androsch, Interdisciplinary Center for Transfer-Oriented Research in Natural Sciences, Martin Luther University Halle-Wittenberg, D-06099 Halle/Saale, Germany

citronellal-polyethylene system. Mapossa et al. [2] made similar assertions for the DEET-polyethylene system but did not provide corroborating evidence. Crystallization-induced solid–liquid phase separation and liquid–liquid phase separation differ with respect to both the transformation kinetics and the resulting microstructure which ultimately controls the repellent release characteristics. It is therefore of great interest to establish the true phase separation mechanism of the DEET-polyethylene system.

Akhtar and Focke [3] achieved a modicum of success establishing the coexistence curves for the citronellal-polyethylene system using hot-stage microscopy in the cooling mode. However, difficulties were experienced with such measurements of the cloud points for mixtures of polyethylene with the mosquito repellent DEET. Theoretical thermodynamic models, which take the differences in molecular size into account, are available. They could assist prediction of the polymer-solvent phase behavior by extrapolation of data gathered for shorter oligomers. The Flory–Huggins theory [12, 13] is an example of such a model that could possibly assist with the prediction of repellent-polyethylene phase behavior from data obtained for shorter chain length linear alkanes. Consequently, attempts were made to determine the location of phase envelopes using differential scanning calorimetry (DSC). This relied on extrapolating demixing onset temperatures obtained at different cooling rates to zero scan rate. Unfortunately, it was found that the enthalpy of demixing in DEET-alkane mixtures was very small and this negatively affected the quality and even the validity of the DSC data.

It is well-established that the composition of liquid mixtures can often be determined from refractive index measurements [14, 15]. The prerequisites are that a calibration curve for refractive index (n) *versus* composition should be available and that it should be a strictly increasing or decreasing function when plotted against either the mole fraction or mass fraction of one of the components. Such a calibration curve would usually only be available at a fixed temperature. The analysis developed in this communication relies on direct estimation of the composition from the measured refractive index of the mixture. With the availability of such a mixing rule [16], this communication describes a novel method of establishing the location of phase envelopes by tracking the refractive index during temperature-scanned cooling experiments. The pure component molar mass and density were obtained and used along with refractive index as a function of temperature to determine the pure component molar refractivity. These values are then used along with the mixture refractive index to calculate the volume fraction of a component present in the mixture. As it cools, the composition locus should either follow the phase boundary or form a jump discontinuity to the other side. The proposed concept was first validated using published data for dimethylacetamide (DMA)-alkane mixtures. Thereafter, the method was applied to mixtures of DEET with a range of linear alkanes of increasing chain length, to finally extrapolate to the phase behavior of polyethylene-DEET mixtures.

2 Theory

Pretorius et al. [16] reviewed the mixing rules proposed for the refractive index (n) of binary mixtures. It was found that the molar refraction for mixtures of linear alkanes with different aromatic or polar compounds behaved like ideal solutions, with both the molar volume (V) and the molar refraction (R) following a linear mixing rule with mole fraction (x_i) as the composition descriptor [16, 17], i.e.,

$$V = V_1x_1 + V_2x_2 \tag{1}$$

and

$$R = R_1x_1 + R_2x_2 \tag{2}$$

where

$$R = V(n^2 - 1)/(n^2 + 2) \text{ and } R_i = V_i(n_i^2 - 1)/(n_i^2 + 2). \tag{3}$$

Combination of Equations (1)–(3) yields a version of the Lorentz–Lorenz mixing rule in terms of volume fraction:

$$\begin{aligned}(n^2 - 1)/(n^2 + 2) =& \varphi_1(n_1^2 - 1)/(n_1^2 + 2) \\ &+ \varphi_2(n_2^2 - 1)/(n_2^2 + 2)\end{aligned} \tag{4}$$

where n is the refractive index of the mixture and n_i and φ_i are the refractive index and volume fraction of component i, respectively.

Numerous studies confirmed that predictions of mixture refractive indices (n) according to the modified Lorentz–Lorenz relationship, i.e., the mixing rule of Equation (4), agree reasonably well with experimental results for many real mixtures [18–21]. The main advantages of implementing this mixing rule are that it is completely predictive and requires only pure component and mixture refractive index data for composition estimates. Pretorius et al. [16] showed that Equation (2) is a significantly more accurate approach for the same purpose.

However, it also requires information on the density of the mixture for which the composition must be established.

It is convenient to define

$$N = (n^2 - 1)/(n^2 + 2) \quad \text{and} \quad N_i = (n_i^2 - 1)/(n_i^2 + 2). \tag{5}$$

Equation (4) can then be solved for the volume fraction of the second component in a form that expresses it in terms of measured N-values as follows:

$$\varphi_2 = (N - N_1)/(N_2 - N_1). \tag{6}$$

Note that the N_i values needed are those obtained at the same temperature as the mixture. The mole fraction can then be determined from the following relationship:

$$x_2 = \varphi_2 V_1/(\varphi_1 V_2 + \varphi_2 V_1). \tag{7}$$

The molar volumes of the pure components are necessary in the application of Equation (7) which implies the need for density data. However, in the absence of information on the effect of temperature on density, good estimates for the molar volumes of the pure components can be obtained using the expression

$$V = M/\rho = R(n^2 + 2)/(n^2 - 1) \tag{8}$$

The utility of Equation (8) arises from the fact that the molar refraction is approximately constant, i.e., temperature independent [16]. Finally, combining these equations, one obtains a simple expression based solely on the measured refractive indices, in combination with the constants R_1 and R_2:

$$x_2 = R_1 N_2 (N - N_1)/[R_1 N_2 (N - N_1) - R_2 N_1 (N - N_2)] \tag{9}$$

It should be noted that the molar refraction combines density and refractive index in a single parameter. It turns out the constancy of the molar refraction R for pure compounds, and the fact that it follows the linear mixing rule for mixtures, results from a mutual compensation effect with temperature: the variations in density are inversely correlated with changes in the refractive index. Therefore, it was found that Equation (2) yields very accurate results for all alkane mixtures considered by Pretorius et al. [16]. Equation (4) also provides accurate data representation for some binaries, for example for the alkane-chlorobenzene mixtures. However, it fails for other systems, in particular for binaries for which the refractive index of a mixture takes on values that are lower than those of the constituents (which is the case for the dioxane-hexane system). Therefore, it is necessary to check the validity of Equation (4) for the system to be studied.

3 Validation using data for dimethylacetamide-alkane mixtures

The DMA-alkane system is used to illustrate the use of Equation (4) because it, like DEET, contains an amide functional group. Furthermore, extensive liquid–liquid equilibrium data have been published for this system [22, 23], with some of it determined by refractive index measurements [24–28]. The latter data was reevaluated using the fully predictive approach outlined above, i.e., applying Equation (4) to estimate composition in terms of volume fractions. If required, the latter can be transformed into mole fractions using Equation (7). The only data used in that approach were the mixture and pure component refractive indices with density data known only for the pure components.

The Xueqin group [24–28] assumed a linear temperature dependence and a polynomial composition dependence for the refractive index of the mixtures of DMA with linear alkanes. They measured refractive index values for the pure compounds and for some homogenous mixtures in order to fix the adjustable constants in their models. For the DMA-hexane binary they assumed quadratic composition dependence equivalent to:

$$n(T, x_1) = n_1 x_1 + 2n_{12} x_1 x_2 + n_2 x_2 + (m_1 x_1 + m_2 x_2)(T - T_o) \tag{10}$$

where n_i is the refractive index of pure component i at the reference temperature T_o; the m_i are the derivatives with respect to temperature of the pure component refractive index curves; and n_{12} is an interaction constant, the only parameter for this binary that uniquely affects the liquid mixture behavior. In effect, Equation (10) implemented a second order Scheffé polynomial to account for the composition dependence of the refractive index at the reference temperature. The model formulation expressed by Equation (10) represents a mathematically equivalent form of the equation which the authors actually implemented.

At first sight, this empirical model appears rather simplistic. It seeks to correlate mixture behavior at the reference temperature with a single adjustable parameter. Temperature dependence is essentially based on a mole fraction-weighted average of the slopes for the pure components stated in Equation (1). Nevertheless, Figure 1 shows that this equation, when applied to the DMA-hexane

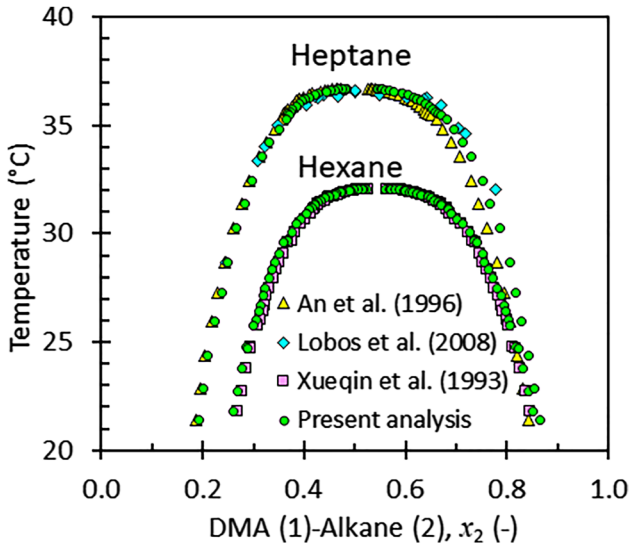

Figure 1: Liquid–liquid phase envelopes for the binary mixture of dimethylacetamide (DMA) with either hexane or with heptane.

system yielded almost identical results as were generated by the joint application of Equations (4) and (7). However, this is not the case for the other systems investigated by the Xueqin group. Figure 1 also shows data for the DMA-heptane system reported by Lobos et al. [22] and by An et al. [28], with the latter study coming from the Xueqin group. Interestingly, reevaluation of their data for heptane according to Equations (4) and (7) led to a better agreement with the data reported by Lobos et al. [22]. Based on these encouraging results, all systems investigated by the Xueqin group were recalculated using the present approach. These were then collated with the data produced by Tristán et al. [23]. The results are presented in Figure 2.

Liquid–liquid phase separation of organic compounds show characteristic features reminiscent of the 3D-Ising model [29]. This is surprising considering the simplicity of the Ising model which just considers entities located on a rigid three-dimensional lattice [30]. These can assume one of two possible states and their interactions are limited to nearest neighbors. Such a system is capable of a phase transition, where the two phases differ with respect to the relative occupation of the two states. These are described by one single order parameter that distinguishes the different phases by assuming nonzero values for ordered states and vanishes when passing through a continuous phase transition.

When applied to liquid–liquid phase separation, the relative occupation of the two states in the Ising model is identified with a suitable composition variable, for example the volume- or the mole fraction. Near the UCST, T_c, the differences in the compositions of the coexisting phases can be represented by a power series in the reduced temperature $\tau = |T - T_c|/T_c$ [31]. Renormalization group theory led to the following expression for the shape of the coexistence curve [32]:

$$z_R - z_L = B\tau^{\beta} + B_1\tau^{\beta+\Delta} + B_2\tau^{\beta+2^{\Delta}} + \ldots \tag{11}$$

where $\beta = 0.326$ and $\Delta = 0.50$ are universal critical exponents [33]; the B_i are system-dependent critical amplitudes; z_c, is the critical value of the composition variable z that defines the order parameter $z_R - z_L$, and the subscripts R and L refer to the right and left branches of the coexistence curve, respectively.

Singh and Pitzer [34] suggested that the amplitude of the first correction-to-scaling term in Equation (11) universally assumes the value $B_1 \approx 0$ in fluid mixtures. Therefore, it is common practice to only retain the leading term in Equation (11), with the others considered negligible and therefore superfluous [30]:

$$z_R - z_L = B\tau^{\beta}. \tag{12}$$

There is a noticeable discrepancy between the Ising phase diagram and those for real binary liquid–liquid systems. Unlike the phase diagrams predicted by the former, those for real fluids are generally asymmetric. The average composition of the two phases, termed the diameter, is not constant but varies with temperature due to this asymmetry. Mean field models, e.g., the van der Waals equation, predict that the diameter of the phase diagram varies linearly with

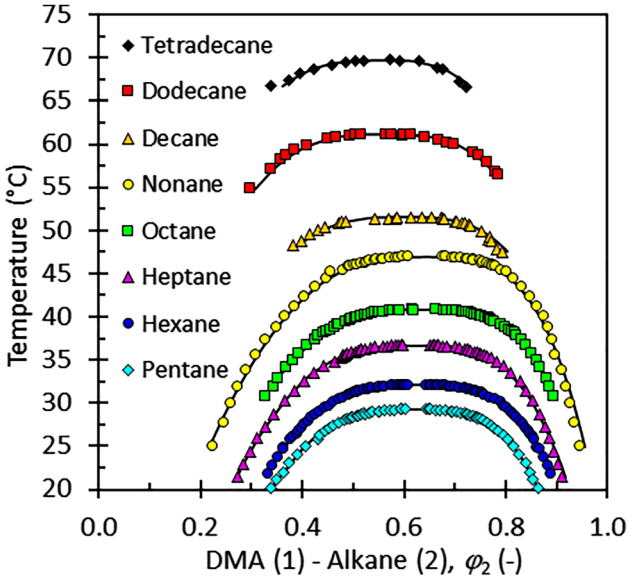

Figure 2: Coexistence curves (φ_1, T) for alkane (1)-DMA (2) systems. Data from the Xueqin group [24–28] for pentane to nonane was re evaluated by applying Equation (4). The data for decane and upward are from Tristan et al. [23]. Solid lines represent least-squares fits using Equation (15).

the temperature near the critical point [29]. This is known as the Cailletet–Mathias rectilinear diameter rule [35]. However, recent theoretical work [36] led to the conclusion that the diameter of the coexistence curve, in general, is a sum of a linear term and nonanalytical terms with critical exponents of $1 - \alpha$ and 2β, respectively, i.e.,

$$d = (z_R + z_L)/2 = z_c + A_o\tau^{1-\alpha} + A_1\tau^{2\beta} + \ldots \quad (13)$$

where $\alpha = 0.110$ is a universal critical exponent and the A_i, are system-dependent critical amplitudes [32].

It is not very clear which order parameter for binary liquid systems is to be preferred, i.e., mole-, mass- or volume fraction [33]. However, Vale et al. [30] pointed out that for different choices of the concentration descriptors, e.g., mole fraction or volume fraction, the relative importance of the terms in Equation (13) varies. Depending on the choice, it may even lead to apparent cancellation of the nonanalytic terms, so that the linear approximation would work well in many instances. Damay and Leclercq [37] noted that the asymmetry of the coexistence curve in binary systems is primarily due to a difference in size between the components. Damay and Leclercq [37] proposed the rescaling of the concentration descriptor in order to achieve a symmetric shape for the phase envelope. If this is possible, it will allow use of Equation (12) only, i.e., it becomes unnecessary to correct for the asymmetry. This proved possible by implementing the q-fractions concept proposed by Wohl [38], i.e., a revised composition variable, defined as follows

$$z_1 = \varphi_1/(\varphi_1 + m\varphi_2) \quad \text{and} \quad z_2 = m\varphi_2/(\varphi_1 + m\varphi_2) \quad (14)$$

where m is an adjustable constant chosen such that the phase envelope, when plotted against z_1, is symmetric and defined by:

$$z_1 = z_c \pm \tfrac{1}{2}B[1 - T/T_c]^{\beta}. \quad (15)$$

This proposal put forward by Damay and Leclercq [37], embodied in Equation (15), was successfully tested using the set of DMA-alkane binaries and subsequently implemented for the DEET-alkane mixtures reported presently.

The thermodynamics of polymers in solution (like polyethylene and DEET) can be described by the Flory–Huggins theory [12, 13]. It is the simplest thermodynamic model that takes differences in molecular size into account. This is due to the fact that it is a lattice model in which it is assumed that each solvent molecule and polymer segment occupy exactly one lattice site with

$$\Delta G_{\text{mix}}/RT = \chi\varphi_1\varphi_2 + \varphi_1\ln\varphi_1 + (\varphi_2/X)\ln\varphi_2 \quad (16)$$

where ΔG_{mix} is the molar Gibbs free energy of mixing per mole of lattice sites; φ_1 and φ_2 are the volume fractions of solvent and polymer respectively; χ is the Flory–Huggins interaction parameter; R is the gas constant; T is the absolute temperature and X is the ratio of the polymer molar volume to that of the solvent:

$$X = \rho_1 M_2/(\rho_2 M_1). \quad (17)$$

UCST phase behavior is well accounted for by the Flory–Huggins theory with the interaction parameter χ exhibiting the following temperature dependence [39]:

$$\chi = A + B/T. \quad (18)$$

where A and B are constants and T is the absolute temperature. The Flory–Huggins theory predicts the following for the critical value of the interaction parameter:

$$\chi_c = 1/2\left[1 + X^{-1/2}\right]^2. \quad (19)$$

The Flory–Huggins theory is unable to represent the phase envelopes in the vicinity of the critical temperature. However, Diekmann et al. [40] indicated that this theory does show the correct trends for the variation of the critical temperature with the molar mass of alkanes. Therefore, these expressions were used to estimate the likely UCST for the DMA-polyethylene combination. The number average molecular mass of the polyethylene considered for making the anklets was 50.4 kDa [3] and these values were used to estimate χ_c for the polymer. Figure 3a shows a plot of χ_c values for the alkane members, as determined from Equation (19) against the inverse of the absolute temperature. The temperature trend agrees with the expectation of Equation (18) for alkanes with chains longer than heptane. Extrapolation to the critical χ_c value for DMA-polyethylene yielded an estimate for the UCST of 185 °C. This temperature is much higher than the melting and crystallization temperature range of the polymer. If this result is reliable, it suggests that at least in some composition range window, the phase separation in the DMA-polyethylene system is likely to occur via liquid–liquid phase separation.

Diekmann et al. [40] suggested an alternative approach for estimating the limiting UCST of a series of alkanes as the molar mass approaches infinity. It is based on the observation that the UCST of the binary mixture correlates strongly with the critical temperature of the alkane. Figure 3b shows this plot for the present alkanes. The values for octane to tetradecane lie on a nearly perfect straight line (correlation coefficient = 0.9995). The latter was extrapolated to the theoretical estimate of $T_{\text{crit}} = 1217$ K for polyethylene reported by Chickos [41]. This estimate was obtained from an indirect method based on the observation that the normal boiling point and the critical point of the polymer converge as the molar mass of the linear alkane approaches infinity. Implementation of this approach resulted in an upper limit estimate for UCST of $T_c = 191$ °C. This value is expected to be only slightly higher than the value of the polyethylene grade considered which obviously

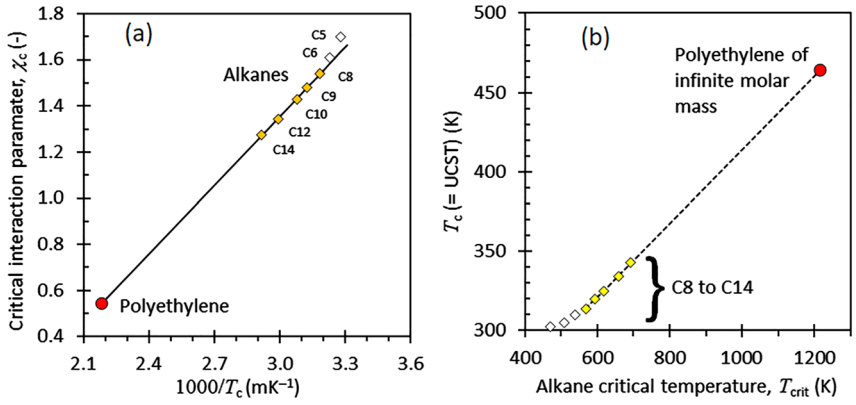

Figure 3: (a) Variation of χ_c *versus* the UCST (T_c) for mixtures of DMA with a series of alkanes estimated from the data reported by [24–28]. The values for octane to tetradecane lie on a straight line with a correlation coefficient equal to 0.9992. The limiting value for the UCST for polyethylene is determined from its χ_c value. (b) Variation of the UCST (T_c) with the critical temperature of the alkane (T_{crit}) in the mixture with DMA. The values for octane to tetradecane lie on a straight line with a correlation coefficient equal to 0.9995. The limiting value for a polyethylene is determined from the estimated theoretical T_{crit} value at infinite molar mass.

does not have an infinite molecular mass. At infinite molar mass, the Flory–Huggins interaction parameter approaches the critical value of $\chi_c = 0.5$ and this yields $T_c = 194$ °C which is surprisingly close to value of 191 °C inferred from the Diekmann et al. [40] approach.

4 Materials and methods

All compounds were obtained from Merck and used as received without further purification. Table 1 lists details about the compounds. Refractive index values were measured as a function of temperature using a Mettler Toledo R4 refractometer. The sample holder is conical with a prism located at the tip in the bottom. It defines the window where the optical measurement is conducted. This means that the refractive index is measured for the layer of fluid in direct contact with the flat surface of the prism (i.e., the densest phase in a phase separated mixture).

The calibration of the instrument was checked using double distilled and deionized water. The instrument precision was ±0.0001 and repeatability was ±0.0002 refractive index units. Sample amounts varied between 0.15 and 0.5 g. They were weighed out and directly placed into the instrument cell where the mixtures were allowed to equilibrate before measurement started.

Table 1: Details and properties of chemicals used.

Alkane	CAS #	mp (°C)	bp (°C)	Purity (%)
DEET (diethyl *m*-toluamide)		−33		
Dodecane (C12)	112-40-3		216	>99
Hexadecane (C16)	544-76-3	18	287	>99
Eicosane (C20)	112-95-8	37		99
Tetracosane (C24)	641-31-1	54	391	99
Octacosane (C28)	630-02-4	61		99
Dotriacontane (C32)	544-85-4	70	467	97

The procedure of generating the phase envelopes is illustrated in Figure 4. The actual experimental procedure was as follows:

- The liquid sample was prepared by accurately weighing out suitable quantities of the two components into the measurement cell.
- The temperature was set at a high value where the mixture is a homogeneous solution.
- The refractive index was measured once the system equilibrated.
- A check was done to justify the validity of the model. For this, the measured refractive index value was compared to the one predicted by Equation (5) using the relationship

$$n_{pred} = [(1 + 2N)/(1 - N)]^{1/2}. \quad (20)$$

- At those temperatures where the solution is homogeneous, the predicted composition should match the set values. If that was the case, the aforementioned assumptions were considered justified.
- The temperature was lowered by a few degrees, and the procedure was repeated.
- The locus of the refractive index, for a homogeneous liquid, follows a straight line if plotted against temperature and, on the temperature-composition plot, it is a vertical line. Once the boundary of a two phase region is traversed, the locus of the measured refractive index deviates from these straight lines because the composition changes. Once this happened, sufficient time was allowed to ensure that the system reached a true equilibrium state. This took several minutes and, in a few cases, it took more than an hour. The molar volume of the DEET was estimated at the measurement temperature using Equation (8). The molar volume of the alkanes being tested was estimated using the density correlations reported by Yaws and Pike [42]. The apparent composition of the mixture was then estimated from the following expressions

$$\varphi_1 = (N - N_2)/(N_1 - N_2) \quad \text{and} \quad x_1 = \varphi_1 V_2/(\varphi_1 V_2 + \varphi_2 V_1). \quad (21)$$

- The temperature was adjusted and the process repeated. On further cooling, the composition locus should hug a phase boundary curve or “jump” to the other branch of the phase envelope on the other side of the critical temperature.

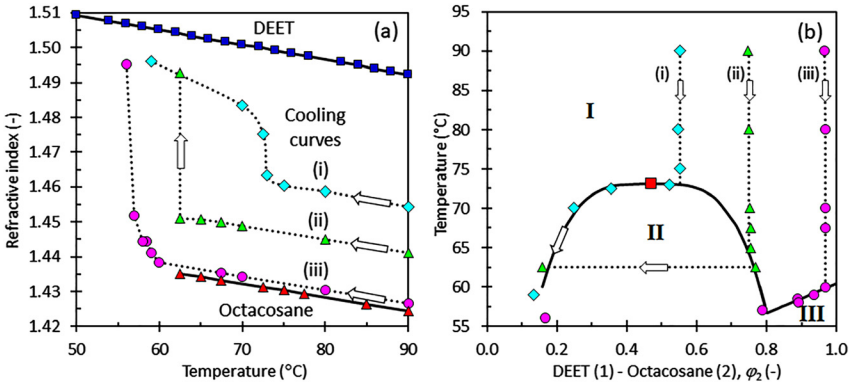

Figure 4: Data for three different mixtures of DEET with octacosane, initially equilibrated as homogeneous solutions at 90 °C. (a) shows the loci of the measured refractive indices as the samples were cooled. Applying Equation (6) transformed this information into the results plotted in (b), which generate an outline of the phase envelopes. The black square in (b) shows the critical temperature at the critical volume fraction.

5 Results and discussion

Table 2 lists the measured refractive index values for DEET and the alkanes, considered presently, in the liquid state. The temperature dependence was almost perfectly linear. Table 2 also lists the slope and intercept for each of the compounds evaluated as well as the measured molar refraction. Dodecane showed the greatest scatter in the value of the latter with the standard deviation amounting to 0.14% of the reported value.

Figure 4 illustrates the experimental procedure used to gather data for the DEET-octacosane system. It shows the cooling results for three different mixtures that started out initially as homogeneous solutions at 90 °C. Figure 4a shows the variation of the refractive indices with temperature for the neat DEET and pure octacosane as solid black lines at the top and bottom of the plot. Figure 4a also shows the trajectories of the refractive indices, in the *n*-temperature plane, while Figure 4b shows the corresponding loci in the temperature-composition plane. Equation (6)

Table 2: Refractive index (*n*) and molar refraction *(R)* values for DEET and selected linear alkanes.

Temperature (°C)	DEET	Dodecane C12	Hexadecane C16	Eicosane C20	Tetracosane C24	Octacosane C28	Dotriacontane C32
15		1.4241					
20	1.5227	1.4219	1.4345				
25		1.4197	1.4325				
30	1.5180	1.4174	1.4305				
35		1.4152	1.4283				
40	1.5134	1.4128	1.4264	1.4344			
45		1.4108	1.4241	1.4324			
50	1.5091	1.4085	1.4221	1.4303			
55		1.4063	1.4199	1.4283			
60	1.5047	1.4041	1.4178	1.4263	1.4319		
65			1.4156	1.4242	1.4299	1.4343	
70	1.5005	1.3995	1.4137	1.4221	1.4279	1.4323	
75		1.3973	1.4114	1.4202	1.4261	1.4303	1.4335
80	1.4959	1.3950	1.4093	1.4181	1.4240	1.4284	1.4316
85			1.4071	1.4167	1.4221	1.4264	1.4296
90	1.4920	1.3904	1.4051	1.4140	1.4201	1.4244	1.4277
95				1.4120	1.4181	1.4224	1.4257
100	1.4876	1.3857	1.4007	1.4099	1.4160	1.4205	1.4238
Correlation coefficient *r* and model constants for $n = n_o + mT$ with temperature in °C							
n_o	1.53109	1.43095	1.44315	1.45063	1.45564	1.45994	1.46270
$m \times 10^4$	−4.3683	−4.5004	−4.2316	−4.0580	−3.9533	−3.9476	−3.8914
r	−0.9998	−1.0000	−1.0000	−0.9997	−0.9999	−1.0000	−1.0000
Molar refraction							
R	58.43	57.86	76.43	95.06	112.89	131.24	149.66
s	–	0.08	0.06	0.04	0.11	0.15	0.04

The constants for the linear correlation with temperature are also listed. *R*, molar refraction; *r*, correlation coefficient; *s*, standard deviation.

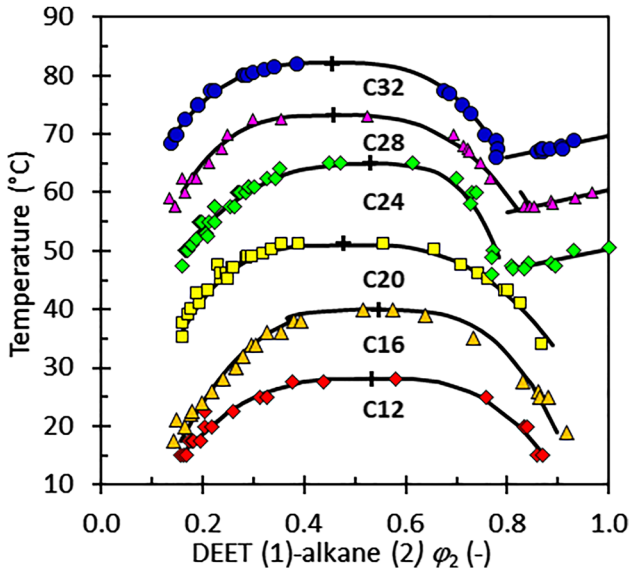

Figure 5: Phase diagram derived from refractive index temperature scans for binary mixtures of DEET with the series of alkanes listed in Table 1. The temperature is plotted against the volume fraction alkane in the mixture.

defined the transformation from Figure 4a to 4b. Note that in Figure 4a, the refractive index loci initially follow straight line paths with slopes intermediate in magnitude to those of the two pure components. These linear sections appear as vertical lines in Figure 4b because they correspond to fixed compositions. However, below a characteristic temperature, each refractive index trajectory shows a sudden deviation from linearity. This is indicative of a change in composition in the liquid being sampled and it is indicative of phase separation.

The trajectories in Figure 4b are shown superimposed on the phase boundaries established on the basis of several additional temperature scans using samples with different starting compositions. They divide the plane into several separate regions. The phase present in Region I corresponds to the homogeneous liquid state. Region II is a two phase zone as the solution has separated into separate liquid phases. Region III corresponds to solid–liquid equilibrium. Here the phase boundary line defines the composition of the liquid in equilibrium with solid octacosane crystals.

As mentioned, the cooling trajectories in Region I of Figure 4b should correspond to vertical lines as the composition of the mixture remains constant. However, once a phase boundary is traversed, a deviation in this trend is observed for the refractive index. This is caused by a change in the composition of the liquid in contact with- and detected by the sensor. If sufficient time is allowed for equilibration, the measured compositions will in fact trace out the location of the phase boundaries in Figure 4b. This happened, for example, for the sample (iii) that contained only a small amount of DEET. It traced out the solid–liquid phase boundary in the region where the octacosane crystallized, i.e., it defined the melting point depression curve. The composition locus for sample (i) traced out the left part of the liquid–liquid phase boundary. Sample (ii) showed a sudden jump from the initial composition to one of a much lower octacosane concentration. Both of these effects are due to gravity. It causes the denser phase to accumulate at the bottom of the cell where the measurement window of the instrument is located.

The phase envelopes for the all the DEET-alkane combinations were determined using the procedure described above. The final results are presented in Figure 5. The UCST (T_c) was determined by curve fitting implementing Equation (15). Estimates for the possible values of the UCST for DEET-polyethylene mixtures were then obtained by implementing the same approach used for the DMA-alkane systems. The results are presented in Table 3 and in Figure 6. Both approaches yielded estimates for the UCST that are well above the melting point range of the polyethylene that was used by Mapossa et al. [2] to prepare mosquito repellent anklets. The implication is that they were correct in assuming that the microporous microstructure resulted from an initial liquid–liquid phase separation.

Table 3: Projected T_c (UCST) values for the DEET-polyethylene system.

Approach/equation	Coefficients		Correlation	UCST	95% confidence interval
Flory–Huggins:	A	B	r	°C	°C
$\chi_c = A + B/T_c$	−1.8958	1.1131	0.9900	183.4	148.0–217.1
Diekmann et al. [40]:	a	b	r	°C	°C
$T_c = a + bT_{crit}$	117.1	0.2762	0.9953	180.1	162.1–198.2

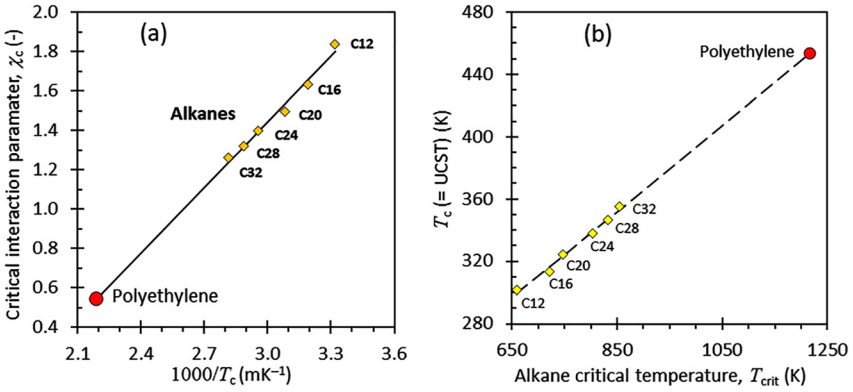

Figure 6: (a) Variation of χ_c *versus* the UCST (T_c) for mixtures of DEET with a series of alkanes. The values for octane to tetradecane lie on a straight line with a correlation coefficient equal to 0.9902. The limiting value for the UCST for polyethylene is determined from its χ_c value as 183.4 °C. (b) Variation of the UCST (T_c) with the critical temperature of the alkane (T_{crit}) in the mixture with DEET. The values for octane to tetradecane lie on a straight line with a correlation coefficient equal to 0.9950. The limiting value for the UCST for a polyethylene is determined from the estimated theoretical T_{crit} value at infinite molar mass as 180.1 °C.

6 Conclusions

A novel method for estimating the UCST of mosquito repellent-polymer systems was developed. Initially, published refractive index data of DMA-alkane systems were reanalyzed to prove that a refractive index mixing rule, linear in volume fraction, allows for adequate composition description of amide-alkane systems. Furthermore, it was shown that asymmetry in the phase envelopes of these systems could be addressed by employing a single adjustable parameter in the composition descriptor, which allows for very good representation of the phase boundaries and subsequent estimation of UCST values. The UCST values of the DMA-alkane systems behaved linearly in the Flory–Huggins critical interaction parameter as well as in alkane critical temperature for alkanes with chain length greater than C7. Extrapolation to estimate UCST values of systems with higher molecular mass components using these parameters was therefore deemed a reasonable approach.

Mixtures of DEET with alkanes of chain length between C12 and C32 were subsequently considered. For each system, the refractive index trajectories of several initially homogenous mixtures were measured upon cooling. Discontinuities from linear behavior were used to signal phase separation. The refractive index measurements of the denser phase were translated into phase diagrams using volume fraction as composition descriptor.

The UCST values obtained by fitting the adjusted composition descriptor model confirmed linear behavior in both the Flory–Huggins critical interaction parameter, as well as the alkane critical temperature for DEET-alkane systems. Extrapolation using the Flory–Huggins approach resulted in an estimate of 183.4 °C for the UCST value of the DEET-polyethylene system, with a 95% confidence interval of between 148.0 and 217.1 °C. The approach that assumes linear behavior in the UCST with the alkane critical temperature yielded an estimated value of 180.1 °C, with a 95% confidence interval between 162.1 and 198.2 °C. Both ranges are significantly above the melting point range of polyethylene (around 126 °C). This confirms that the previously reported microporous microstructure of mosquito repellent materials, formed from the DEET-polyethylene system by using TIPS, is a result of an initial liquid–liquid phase separation and not polymer crystallization.

Author contributions: All the authors have accepted responsibility for the entire content of this submitted manuscript and approved submission.
Research funding: Financial support from the Deutsche Forschungsgemeinschaft (DFG), under grant AN 212/22-2, is gratefully acknowledged.
Conflict of interest statement: The authors declare no conflicts of interest regarding this article.

References

1. Sibanda M., Focke W., Braack A., Leuteritz A., Brünig H., An Tran N. H., Wieczorek F., Trümper W. Bicomponent fibres for controlled release of volatile mosquito repellents. *Mater. Sci. Eng. C Mater. Biol. Appl.* 2017, *91*, 754–761.
2. Mapossa A. B., Sibanda M. M., Sitoe A., Focke W. W., Braack L., Ndonyane C., Mouatcho J., Smart J., Muaimbo H., Androsch R., Loots M. T. Microporous polyolefin strands as controlled-release devices for mosquito repellents. *Chem. Eng. J.* 2019, *360*, 435–444.
3. Akhtar M. U., Focke W. W. Trapping citronellal in a microporous polyethylene matrix. *Thermochim. Acta* 2015, *613*, 61–65.

4. Castro A. J. *Methods for Making Microporous Products*. US 4247498 A, 1981.
5. Lloyd D. R., Kinzer K. E., Tseng H. S. Microporous membrane formation via thermally induced phase separation. I. Solid-liquid phase separation. *J. Membr. Sci.* 1990, *52*, 239–261.
6. Ulbricht M. Advanced functional polymer membranes. *Polymer* 2006, *47*, 2217–2262.
7. Sungkapreecha C., Iqbal N., Focke W. W., Androsch R. Crystallization of poly(l-lactic acid) in solution with the mosquito-repellent N,N-diethyl-3-methylbenzamide. *Polym. Cryst.* 2019, *2*, e10029.
8. Sungkapreecha C., Focke W. W., Androsch R. Competition between liquid-liquid de-mixing, crystallization, and glass transition in solutions of PLA of different stereochemistry and DEET. *Chin. J. Polym. Sci.* 2020, *38*, 174–178.
9. Sungkapreecha C., Beily M. J., Kressler J., Focke W. W., Androsch R. Phase behavior of the polymer/drug system PLA/DEET: effect of PLA molar mass on subambient liquid-liquid phase separation. *Thermochim. Acta* 2018, *660*, 77–81.
10. Sungkapreecha C., Iqbal N., Gohn A. M., Focke W. W., Androsch R. Phase behavior of the polymer/drug system PLA/DEET. *Polymer* 2017, *126*, 116–125.
11. Yener H. E., Hillrichs G., Androsch R. Phase behavior of solvent-rich compositions of the polymer/drug system poly(butylene succinate) and N,N-diethyl-3-methylbenzamide (DEET). *Colloid Polym. Sci.* 2021, *299*, 873–881.
12. Flory P. J. Thermodynamics of high polymer solutions. *J. Chem. Phys.* 1941, *9*, 660–661.
13. Huggins M. L. Solutions of long chain compounds. *J. Chem. Phys.* 1941, *9*, 440.
14. Martens M., Hadrich M. J., Nestler F., Ouda M., Schaadt A. Combination of refractometry and densimetry – a promising option for fast raw methanol analysis. *Chem. Ing. Tech.* 2020, *92*, 1474–1481.
15. Shehadeh A., Evangelou A., Kechagia D., Tataridis P., Chatzilazarou A., Shehadeh F. Effect of ethanol, glycerol, glucose/fructose and tartaric acid on the refractive index of model aqueous solutions and wine samples. *Food Chem*. 2020, *329*, 127085.
16. Pretorius F., Focke W. W., Androsch R., du Toit E. L. Estimating binary liquid composition from density and refractive index measurements: a comprehensive review of mixing rules. *J. Mol. Liq.* 2021, *332*, 115893.
17. Brocos P., Piñeiro Á., Bravo R., Amigo A. Refractive indices, molar volumes and molar refractions of binary liquid mixtures: concepts and correlations. *Phys. Chem. Chem. Phys.* 2003, *5*, 550–557.
18. Heller W. Remarks on refractive index mixture rules. *J. Phys. Chem.* 1965, *69*, 1123–1129.
19. Tasic A. Z., Djordjevic B. D., Grozdanic D. K., Radojkovic N. Use of mixing rules in predicting refractive indexes and specific refractivities for some binary liquid mixtures. *J. Chem. Eng. Data* 1992, *37*, 310–313.
20. Krishnaswamy R. K., Janzen J. Exploiting refractometry to estimate the density of polyethylene: the Lorentz–Lorenz approach re-visited. *Polym. Test.* 2005, *24*, 762–765.
21. Iglesias-Otero M. A., Troncoso J., Carballo E., Romaní L. Density and refractive index in mixtures of ionic liquids and organic solvents: correlations and predictions. *J. Chem. Thermodyn.* 2008, *40*, 949–956.
22. Lobos J., Mozo I., Regúlez M. F., González J. A., García de la Fuente I., Cobos J. C. Thermodynamics of mixtures containing a strongly polar compound. 8. Liquid–liquid equilibria for N,N-dialkylamide + selected N-alkanes. *J. Chem. Eng. Data* 2006, *51*, 623–627.
23. Tristán C. A., González J. A., García De La Fuente I., Cobos J. C. Thermodynamics of mixtures containing a very strongly polar compound. 10. Liquid–liquid equilibria for N,N-dimethylacetamide + selected alkanes. *J. Chem. Eng. Data* 2013, *58*, 2339–2344.
24. Xueqin A., Weiguo S., Haijun W., Guokang Z. The (liquid+liquid) critical phenomena of (a polar liquid+an n-alkane). I. Coexistence curves of (N,N-dimethylacetamide+hexane). *J. Chem. Thermodyn.*1993, *25*, 1373–1383.
25. Xueqin A., Weiguo S. The (liquid + liquid) critical phenomena of (a polar liquid + an n-alkane) II. Coexistence curves of (N,N-dimethylacetamide + octane). *J. Chem. Thermodyn.* 1994, *26*, 461–468.
26. Xueqin A., Haihong Z., Weiguo S. The (liquid + liquid) critical phenomena of (a polar liquid + ann-alkane): III. Coexistence curves of (N, N-dimethylacetamide + pentane). *J. Chem. Thermodyn.* 1995, *27*, 1241–1247.
27. Xueqin A., Haihong Z., Weiguo S. The (liquid + liquid) critical phenomena of (a polar liquid + an n-alkane) IV. Coexistence curves of (N,N-dimethylacetamide + nonane). *J. Chem. Thermodyn.* 1996, *28*, 1165–1172.
28. An X., Zhao H., Jiang F., Shen W. The (liquid + liquid) critical phenomena of (a polar liquid + ann-alkane) V. Coexistence curves of (N,N-dimethylacetamide + heptane). *J. Chem. Thermodyn.* 1996, *28*, 1221–1232.
29. Domb C. *The Critical Point: A Historical Introduction to the Modern Theory of Critical Phenomena*; CRC Press: Boca Raton, LA, 1996.
30. Vale V. R., Rathke B., Will S., Schröer W. Liquid–liquid phase behavior of solutions of 1-dodecyl-3-methylimidazolium bis((trifluoromethyl)sulfonyl)amide (C12mimNTf2) in *n*-alkyl alcohols. *J. Chem. Eng. Data* 2010, *55*, 4195–4205.
31. Schröer W., Vale V. R. Liquid-liquid phase separation in solutions of ionic liquids: phase diagrams, corresponding state analysis and comparison with simulations of the primitive model. *J. Phys. Condens. Matter* 2009, *21*, 424119.
32. Aizpiri A. G., Monroy F., del Campo C., Rsubio R. G., Díaz Peña M. Range of simple scaling and critical amplitudes near a LCST. The 2-butoxyethanol + water system. *Chem. Phys.* 1992, *165*, 31–39.
33. Kumar A., Krishnamurthy H. R., Gopal E. S. R. Equilibrium critical phenomena in binary liquid mixtures. *Phys. Rep.* 1983, *98*, 57–143.
34. Singh R. R., Pitzer K. S. Relationships in the approach to criticality in fluids, including systematic differences between vapor-liquid and liquid-liquid systems. *J. Chem. Phys.* 1989, *90*, 5742–5748.
35. Reif-Acherman S. The history of the rectilinear diameter law. *Quím. Nova* 2010, *33*, 2003–2010.
36. Cerdeiriña C. A., Anisimov M. A., Sengers J. V. The nature of singular coexistence-curve diameters of liquid–liquid phase equilibria. *Chem. Phys. Lett.* 2006, *424*, 414–419.
37. Damay P., Leclercq F. Asymmetry of the coexistence curve in binary systems. Size effect. *J. Chem. Phys.* 1991, *95*, 590–599.
38. Wohl K. Thermodynamic evaluation of binary and ternary liquid systems. *Trans. Am. Inst. Chem. Eng.* 1946, *42*, 215–249.

39. McGuire K. S., Laxminarayan A., Lloyd D. R. A simple method of extrapolating the coexistence curve and predicting the melting point depression curve from cloud point data for polymer-diluent systems. *Polymer* 1994, *35*, 4404–4407.
40. Diekmann S., Dederer E., Charmeteau S., Wagenfeld S., Kiefer J., Schröer W., Rathke B. Revisiting the liquid–liquid phase behavior of n-alkanes and ethanol. *J. Phys. Chem. B* 2020, *124*, 156–172.
41. Chickos J. S. Hypothetical Thermodynamic Properties: the boiling and critical temperatures of polyethylene and polytetrafluoroethylene. *J. Chem. Eng. Data* 2004, *49*, 518–526.
42. Yaws C. L., Pike R. W. Chapter 3 - Density of liquid—organic compounds. In *Thermophysical Properties of Chemicals and Hydrocarbons*; Yaws C. L., Ed.; William Andrew Publishing: Norwich, NY, 2009.